The 3-dimensional zone of the center of resistance of the mandibular posterior teeth segment

Moon-Bee Oh,[a] Sung-Seo Mo,[b] Chung-Ju Hwang,[c] Chooryung Chung,[d] Ju-Man Kang,[e] and Kee-Joon Lee[c]
Seoul, Korea

Introduction: We sought the 3-dimensional (3D) zone of the center of resistance (ZCR) of mandibular posterior teeth groups (group 1: first molar; group 2: both molars; group 3: both molars and second premolar; group 4: both molars and both premolars) with the use of 3D finite element analysis. **Methods:** 3D finite element models comprised the mandibular posterior teeth, periodontal ligament, and alveolar bone. In the symmetric bilateral model, a 100-g midline force was applied on a median sagittal plane at 0.1-mm intervals to determine the anteroposterior and vertical positions of the ZCR (where the applied force induced translation). The most reliable buccolingual position of the ZCR was then determined in the unilateral model. The combination of the anteroposterior, vertical, and buccolingual positions was defined as the ZCR. **Results:** The ZCRs of groups 1-4 were, respectively, 0.48, 0.46, 0.50, and 0.53 of the mandibular first molar root length from the alveolar crest level and located slightly distobuccally at anteroposterior ratios of 2:3.0, 2:2.3, 2:2.4, and 2:2.5 to each sectional arch length and at buccolingual ratios of 2:1.5, 2:1.1, 2:1.6, and 2:2.4 to the first molar's buccolingual width. **Conclusions:** The ZCR can be a useful reference for 3D movement planning of mandibular posterior teeth or segments. (Am J Orthod Dentofacial Orthop 2019;156:365-74)

Mandibular molar movement is regarded as a challenging task for clinicians because of wide root surfaces, the density of the mandibular bone, and significant anchorage demands.[1-3] However, in recent years, the use of temporary anchorage devices (TADs) has enabled various movements of the mandibular molars,[1,4-8] such as protraction, distalization, intrusion, and buccolingual movement, and posterior teeth can be moved not only individually, but also in segments. In this way, the nonsurgical treatment of Class II and III malocclusion and open bite has become possible. Although the use of TADs allows for various movements of the mandibular molars, however, the movement of roots in parallel remains biomechanically difficult without knowledge of the 3-dimensional (3D) center of resistance (CR) of a tooth.

The primary aim of orthodontic treatment is to apply a 3D loading system that prescribes a force to a tooth according to the rules of biomechanics; this requires knowledge of the 3D-CR of a tooth. If the applied force vector passes through the 3D-CR of the tooth, pure translation is possible.[9,10] Once the 3D-CR is located, a more accurate 3D treatment plan can be established. Moreover, as orthodontics shifts into 3D technology and tooth movement planning, the knowledge of biomechanics also needs to be updated. Therefore, it is essential to know the 3D-CR of the mandibular posterior teeth to plan pure translation.

Recent studies reported that the location of the CR depends on the direction of load application.[11,12] In this regard, Viecilli et al[13] suggested a 3D theory of axes of resistance that do not intersect and stated that the CR could be constructed in 3D space not as a point,

[a]Department of Orthodontics, College of Dentistry, Graduate School of Yonsei University, Seodaemun-gu, Seoul, Korea.
[b]Division of Orthodontics, Department of Dentistry, Saint Paul's Hospital, College of Medicine, Catholic University of Korea, Dongdaemun-gu, Seoul, Korea.
[c]Institute of Craniofacial Deformity, Department of Orthodontics, College of Dentistry, Yonsei University, Seodaemun-gu, Seoul, Korea.
[d]Department of Orthodontics, Gangnam Severance Dental Hospital, Gangnam-gu, Seoul, Korea.
[e]Division of Orthodontics, Department of Dentistry, Seoul Saint Mary's Hospital, College of Medicine, Catholic University of Korea, Seocho-gu, Seoul, Korea.
All authors have completed and submitted the ICMJE Form for Disclosure of Potential Conflicts of Interest, and none were reported.
Funding: This research was supported by Basic Science Research Program through the National Research Foundation of Korea (NRF) funded by the Ministry of Education (NRF-2017R1D1A1B03035435).
Address correspondence to: Kee-Joon Lee, Professor, Department of Orthodontics, Institute of Craniofacial Deformity, College of Dentistry, Yonsei University, 50-1 Yonsei-ro, Seodaemun-gu, Seoul, 03722, Korea; e-mail, orthojn@yuhs.ac.
Submitted, May 2018; revised and accepted, October 2018.
0889-5406/$36.00

https://doi.org/10.1016/j.ajodo.2018.10.017

but as a small 3D volume. Therefore, the term "zone of the center of resistance" (ZCR) was introduced in the present study to express that small 3D-CR volume which is our focus.

Most studies[14-17] on the CR have focused on the maxillary anterior teeth, which have been the main targets of tooth movement in orthodontic treatment in the past. With the development of TADs and 3D digital technology, more recent studies have analyzed the CR of the maxillary posterior teeth and the entire dentition with the use of 3D finite element analysis (FEA),[18-20] but very few studies have localized the CR of the mandibular dentition.[21] Furthermore, for mandibular posterior individual teeth or segments, no reports have clarified the ZCR.

Various methods have been used to investigate the CR, such as the laser holography,[14] laser reflection,[15] photoelasticity,[16] electrical resistance strain gauge,[17] and FEA.[18-21] Among these, FEA involves modeling the anatomic structure and physical properties of an object with the use of a computer program and analyzing the deformation and stress distribution of the object with respect to external force. Previous studies have used relatively simple models, but recently, the development of computer software and 3D laser scanning have made it possible to produce more sophisticated finite element models consisting of teeth, periodontal ligaments (PDLs), and alveolar bone for more accurate analyses.[14]

The objective of the present study was to localize the ZCR of 4 groups of mandibular posterior teeth with the use of 3D-FEA.

MATERIAL AND METHODS

A 3D finite element model, composed of the mandibular posterior teeth, PDL, and alveolar bone, was created ensuring left-right symmetry, with the use of the method described by Jo et al[21] (Fig 1). The specific method was as follows.

The outline of the teeth was obtained via 3D laser scanning of the mandibular right posterior teeth of the Nissin teeth model (Model i21D-400G; Nissin Dental Products, Kyoto, Japan), which was created via a sampling study of adults with normal occlusion. The dental arch form was arranged with reference to the broad arch form of Ormco (Glendora, Calif), and the inclination and angulation of each tooth were arranged without the Spee curve and Wilson curve.[21] The thickness of the PDL was assumed to be uniform (0.2 mm) according to the studies by Coolidge[22] and Kronfeld.[23] The alveolar bone was formed along the curvature of the cementoenamel junction (CEJ), at a distance of 1 mm below the CEJ.[24] In the 3D finite element model, the teeth, alveolar bone, and PDL were composed of tetrahedral elements with 4 nodes (Fig 1, *C*), and the finite element model contained 359,970 elements and 71,240 nodes. The teeth were in contact with each other through the contact point as an independent object connected by buccal and lingual splint wires, which were set as a rigid body.

In this study, the teeth, alveolar bone, and PDL were assumed to be homogeneous, isotropic, and linear elastic materials, and the material properties were adopted from previous studies (Table I).[21,25,26] Considering that the roots are primarily and entirely surrounded by cortical bone, the property of the bone was set at 2,000 MPa, to mimic the characteristic of cortical bone.[21] The ANSYS 12.1 program (Swanson Analysis System, Canonsburg, Pa) was used for FEA.

The midpoint of the line of intersection between the distal surface plane of both mandibular second molars and the occlusal plane was set as the origin, the buccolingual (BL) direction as the X-axis, the anteroposterior (AP) direction as the Y-axis, and the vertical direction as the Z-axis. The direction of the buccal side was defined as + X, the anterior direction as + Y, the apical direction as −Z, the YZ plane as the median sagittal plane, and the XY plane as the occlusal plane (Fig 1).

The mandibular posterior teeth groups were classified into 4 types as follows: group 1, the first molar; group 2, the first and second molars; group 3, the first and second molars and second premolar; and group 4, the first and second molars and first and second premolars.

All teeth of each group were splinted by a rigid wire, a virtual rigid body that had no properties of deformation with respect to an external force, on the buccal and lingual side to restrict elastic deformation and 3D distortion, so that each group of teeth moved without individual tooth movement. In addition, in the bilateral symmetric model, the wires cross-linking the left and right teeth and the rigid wire beams extending from the origin in the +Y direction and −Z direction were designed to distribute the applied force evenly to the teeth (Fig 2).

To localize the ZCR, first, in the symmetric bilateral model, an intrusive force (−Z direction) and a distal force (−Y direction) of 100 g were applied to each group along the Y-axis and Z-axis, to determine the AP and vertical positions of the ZCR, respectively (Fig 3, *A*). The combination of the AP and vertical positions was assumed to reflect the 2D-CR projection of the ZCR on the YZ plane. Then, in the unilateral model, to determine the BL position of the ZCR, an intrusive force (−Z direction) of 100 g was applied along the virtual line (+X′) that ran orthogonal to the YZ plane and passed through the 2D-CR (Fig 3, *B*). A force was initially applied at

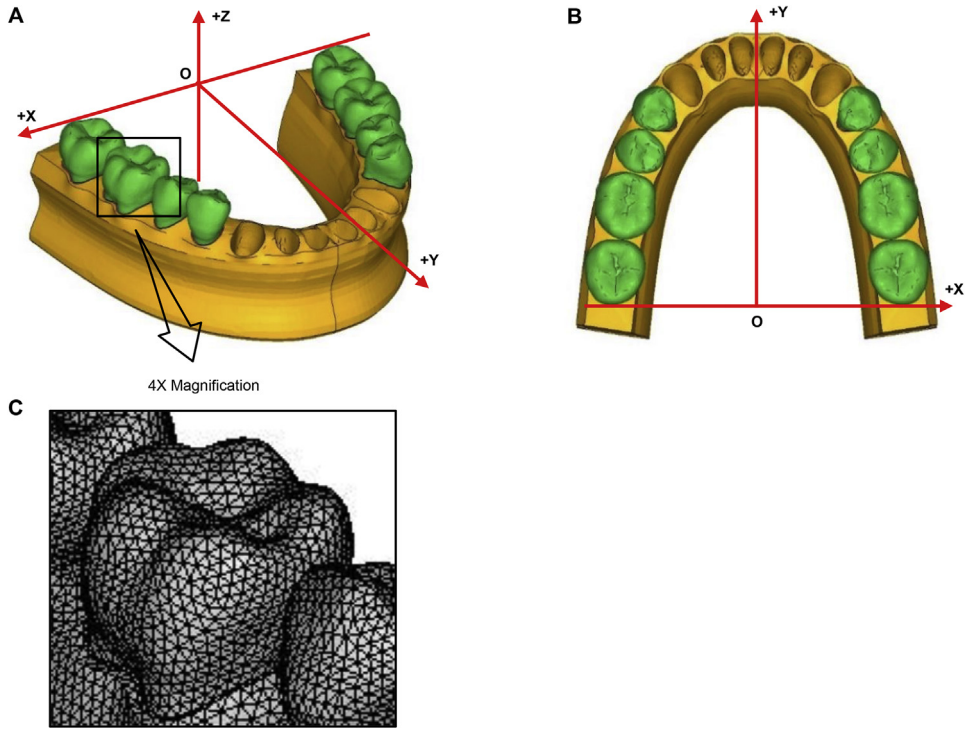

Fig 1. 3D finite element model and schematic representation of the coordinate system used in this study: **A,** oblique view; **B,** occlusal view; **C,** 3D meshing condition of the finite element model

Table I. Material properties of the finite element model

Element	*Young modulus (MPa)*	*Poisson ratio*
Periodontal ligament	5.0E−02	0.49
Alveolar bone	2.0 E+03	0.30
Teeth	2.0 E+04	0.30

intervals of 5 mm to find the reversal position, where the direction of segmental rotation changed. Then, within the range of reversal, reiteration was subsequently performed at intervals of 1 mm, followed by intervals of 0.1 mm.

To investigate the displacement pattern of teeth, specific nodal points (contact point, root apex, and cusp tip) were selected as landmarks for each tooth, and the displacement of a landmark in 3 directions (X-axis, Y-axis, and Z-axis) was expressed as ΔX, ΔY, and ΔZ, respectively. The position where force application moved all teeth of each group in the most parallel manner possible was defined as the ZCR in this study.

The point of force application where the standard deviation (SD) of the vertical displacements (ΔZ) of the (mesio)buccal cusp tips of all teeth belonging to each group was close to zero was defined as the AP position of the ZCR. Exceptionally, for group 1 the force application point where the SD of the ΔZ of the mesiobuccal cusp tip and the mesial root apex was close to zero was defined as the AP position of the ZCR.

The value obtained by subtracting the AP displacement (ΔY) of the (mesio)buccal cusp tip from the ΔY of the (mesial) root apex of each tooth was defined as the differential displacement. The force application point where the sum of the differential displacements of all teeth belonging to the teeth group was close to zero was defined as the vertical position of the ZCR.

The value obtained by subtracting the ΔZ of the (mesio)buccal cusp tip from the ΔZ of the (disto)lingual cusp tip of each tooth was defined as the differential displacement. The point of force application where the sum of the differential displacements of all teeth belonging to the teeth group was close to zero was defined as the BL position of the ZCR. Finally, the area defined by the AP, vertical, and BL positions was defined as the ZCR.

After localizing the ZCR as described above, additional experiments were performed on group 1 in the other loading directions. To analyze the AP and vertical

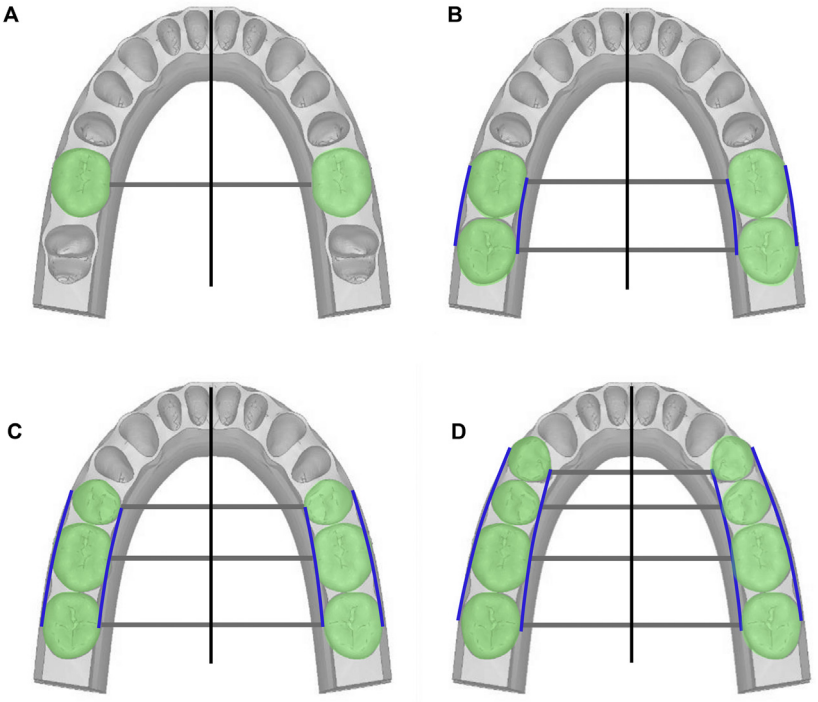

Fig 2. Schematic representation of the finite-element models of the 4 teeth groups in the bilateral symmetric model: **A,** group 1; **B,** group 2; **C,** group 3; **D,** group 4. All teeth of each group were splinted with the use of rigid wire (*blue*) on both the buccal and lingual sides to limit the movement of an individual tooth. The wires (*gray*) cross-linking the left and right teeth and the wire beams (*black*) extending from the origin in the +Y direction and −Z direction were designed to distribute the applied force evenly to the teeth.

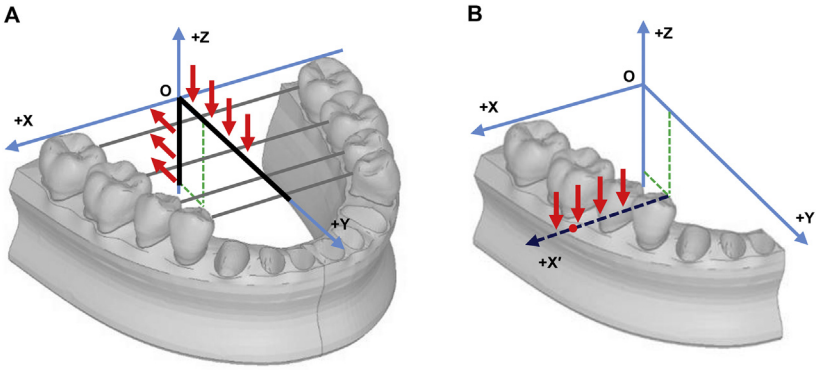

Fig 3. Diagram of the force application method for determining the zone of the center of resistance (ZCR). **A,** Determination of the anteroposterior (AP) and vertical positions of the ZCR in the symmetric bilateral model: Intrusive force (−Z direction) and distal force (−Y direction) were respectively applied along the black-colored wire corresponding to the Y-axis and Z-axis. **B,** Determination of the BL position of the ZCR in the unilateral model: Intrusive force (−Z direction) was applied along the virtual line (+X′) orthogonal to the YZ plane and passed through the 2D center of resistance (the combination of the AP and vertical positions).

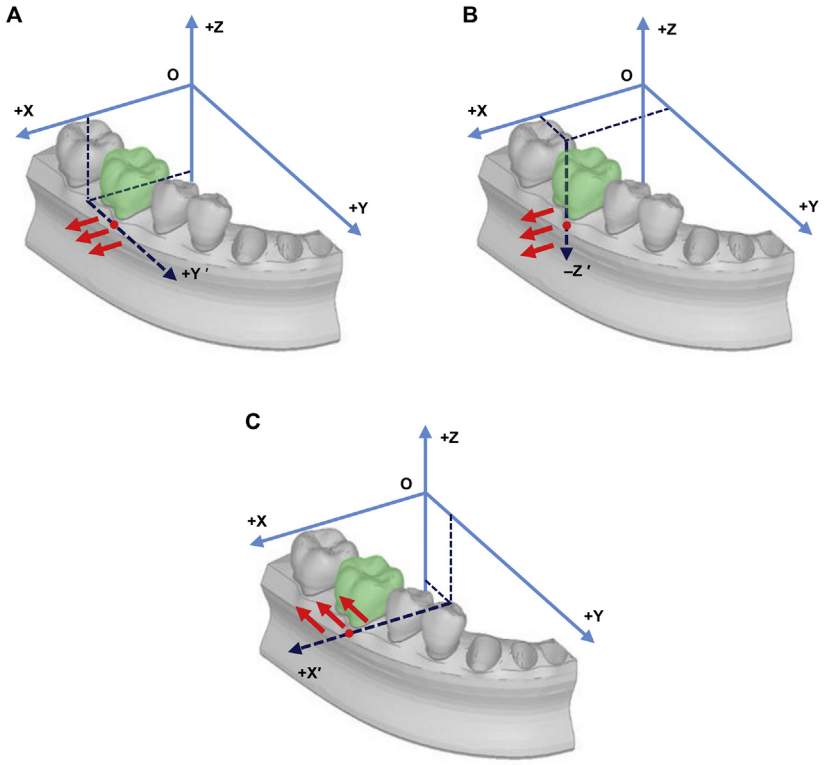

Fig 4. Diagram of the force application method of additional experiments on a mandibular molar to quantify the discrepancies among the 2D centers of resistance (CRs) depending on the loading directions (anteroposterior [AP], vertical, and buccolingual [BL] directions): **A,** determination of the AP position of the 2D-CR in the BL loading direction; **B,** determination of the vertical position of the 2D-CR in the BL loading direction; **C,** determination of the vertical position of the 2D-CR in the AP loading direction.

positions of the 2D-CR in the BL loading direction, an expansional force (+X direction) of 100 g was applied at intervals of 0.1 mm within the ±0.5 mm section near the ZCR, along the virtual line (+Y′/−Z′) that was orthogonal to the XZ plane/XY plane and passed through the ZCR, respectively (Fig 4, *A* and *B*). Furthermore, for analysis of the BL position of the 2D-CR in the AP loading direction, a distal force (−Y direction) of 100 g was applied along the virtual line (+X′) that ran orthogonal to the YZ plane and passed through the ZCR (Fig 4, *C*). The analysis method was as described above.

RESULTS

The ZCR of group 1 was located 4.8 mm (40.3% of the mesiodistal [MD] width) mesial to the distal margin and 12.3 mm (67.9% of the tooth length) apical to the occlusal plane. It was 5.3 mm (48% of the root length) apical to the alveolar crest level, and 2.3 mm below the furcation in the model. It measured 52% of the root length to the CEJ, 6.2 mm (57.4% of the BL width) buccal to the lingual surface, and 2.1 mm (17.6% of MD width) distal and 1.3 mm buccal (12% of the BL width) to the central pit of the first molar (Figs 5 and 6, *A*).

The ZCR of group 2 was located 10.8 mm (45.9% of the sectional arch length) mesial to the distal margin of the second molar. It was 12.1 mm (66.9% of the tooth length of the first molar) apical to the occlusal plane, 5.1 mm (46% of the root length of the first molar) apical to the alveolar crest level, and 6.9 mm (63.9% of the BL width of the first molar) buccal to the lingual surface of the first molar. And it was 7.7 mm (64.7% of the MD width of the first molar) distal and 2 mm (18.5% of the BL width of the first molar) buccal to the central pit of the first molar (Figs 5 and 6, *B*).

The ZCR of group 3 was located 14.1 mm (45.3% of the sectional arch length) mesial to the distal margin of the second molar. It was 12.6 mm (69.1% of the tooth length of the first molar) apical to the occlusal plane, 5.6 mm (50% of the root length of the first molar) apical

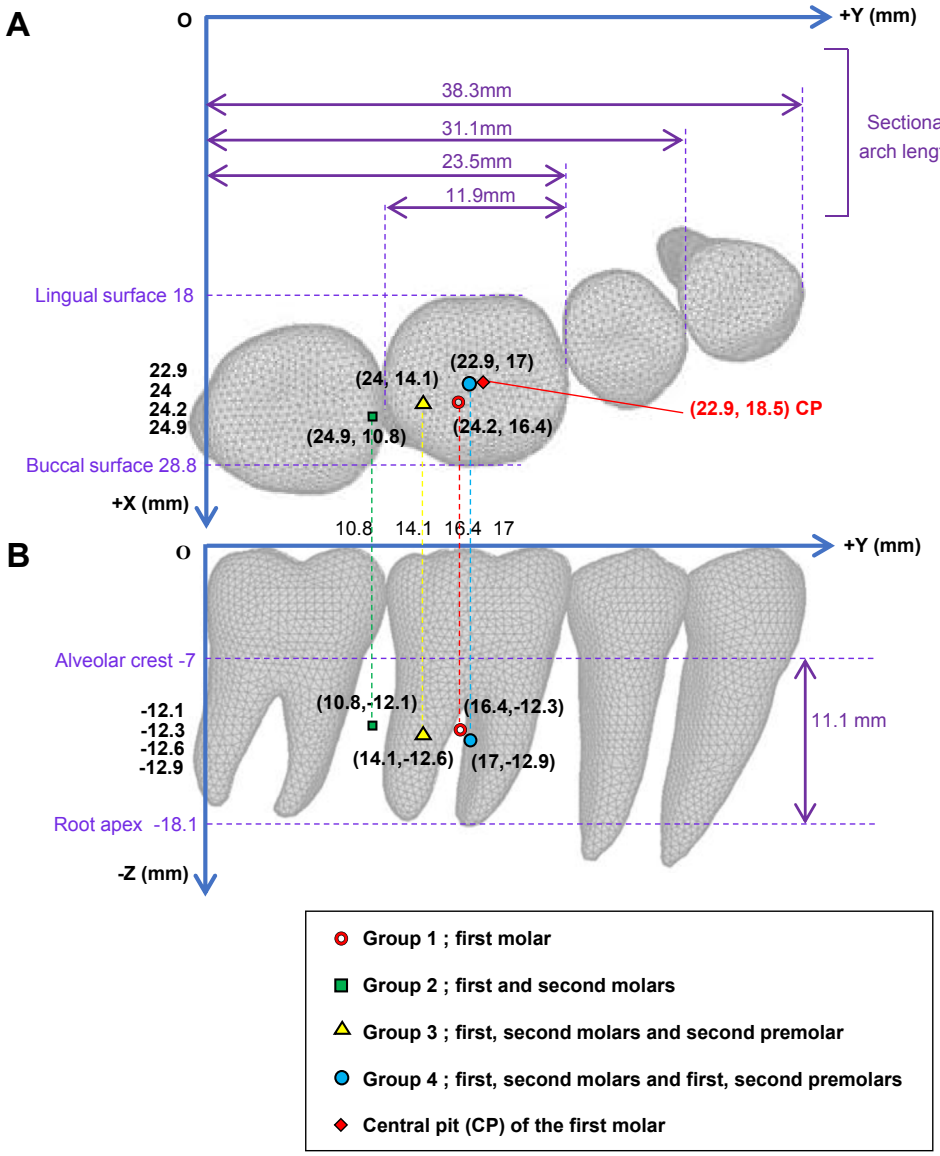

Fig 5. Projections of the coordinate system (*blue*) and the locations of the zones of the center of resistance of the mandibular posterior teeth segments: **A,** occlusal view; **B,** lateral view.

to the alveolar crest level, and 6 mm (55.6% of the BL width of the first molar) buccal to the lingual surface of the first molar. And it was 4.4 mm (37% of the MD width of the first molar) distal and 1.1 mm (10.2% of the BL width of the first molar) buccal to the central pit of the first molar (Figs 5 and 6, *C*).

The ZCR of group 4 was located 17 mm (44.4% of the sectional arch length) mesial to the distal margin of the second molar. It was 5.4 mm (50% of the MD width of the first molar) mesial to the distal margin of the first molar, 12.9 mm (71.3% of the tooth length of the first molar) apical to the occlusal plane, 5.9 mm (53% of the root length of the first molar) apical to the alveolar crest level, and 4.9 mm (45.4% of the BL width of the first molar) buccal to the lingual surface of the first molar. And it was 1.5 mm (12.6% of the MD width of the first molar) distal to the central pit of the first molar (Figs 5 and 6, *D*).

For a mandibular molar, the 2D CR in the BL loading direction was located 12.1 mm apical to the occlusal plane and 5 mm mesial to the distal margin, and the BL position of the 2D CR in the AP loading direction was located 6.3 mm buccal to the lingual surface. The differences among the 2D-CRs depending on the loading directions were only 0.1-0.2 mm in the model (Table II).

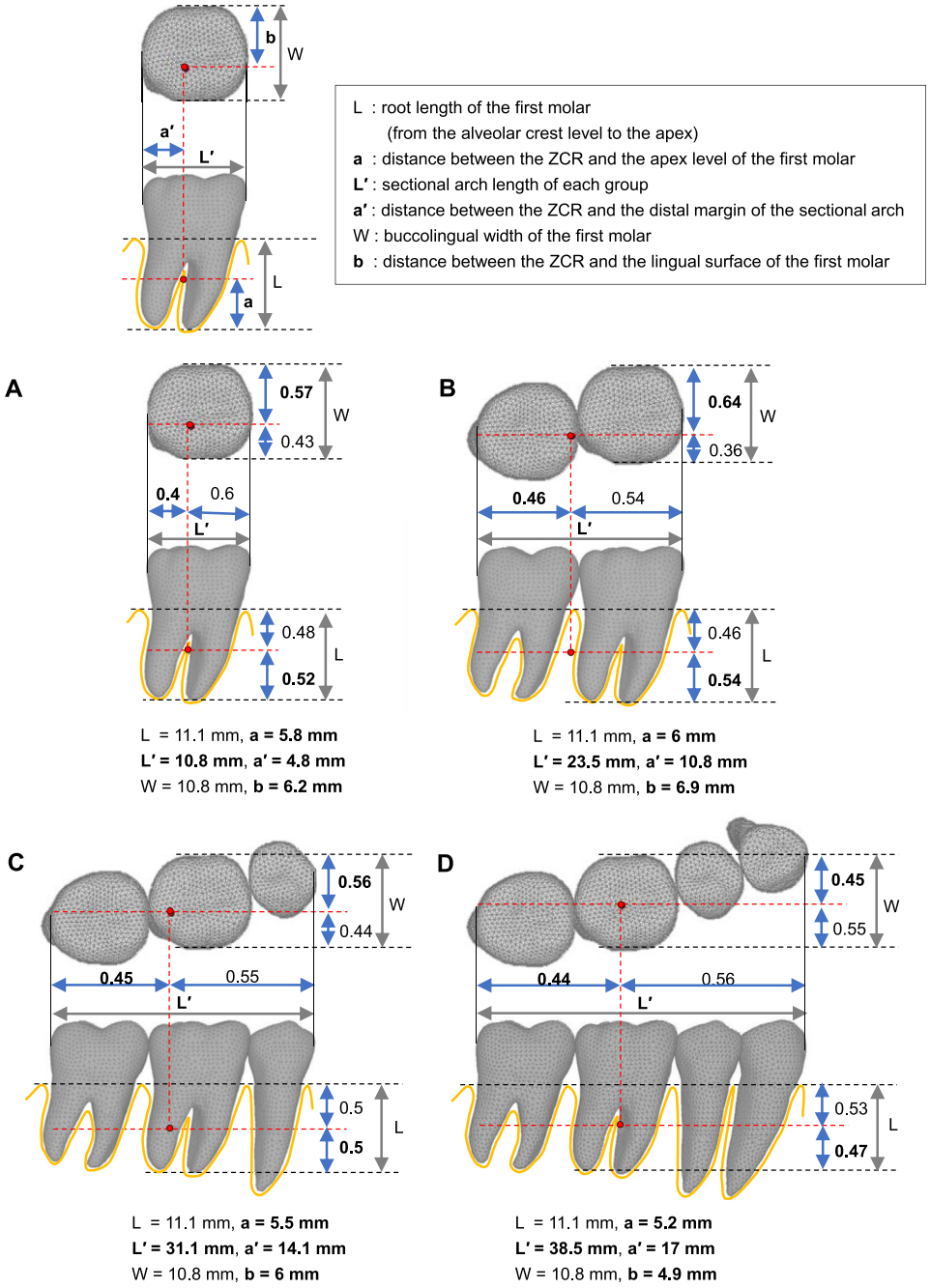

Fig 6. The relative locations of the zones of the center of resistance (ZCRs) of the mandibular posterior teeth segments: **A,** group 1; **B,** group 2; **C,** group 3; **D,** group 4. The location of the ZCR of each group was expressed as a ratio to each reference value (root length [L] and buccolingual width [W] of the mandibular first molar and sectional arch length [L′]).

DISCUSSION

With advances in 3D technology, such as cone-beam computed tomography, 3D laser scanners, and 3D printers, 3D diagnosis and treatment planning has recently become possible in orthodontic treatment. Therefore, establishment of a 3D concept of tooth movement biomechanics is required. In particular, it is essential to know the ZCR of the tooth to apply a more precise 3D loading system. In this study, 3D-FEA was used as a

Table II. Discrepancies among the 2D-CRs of a mandibular molar depending on the loading directions

	Location of the 2D-CR (on the plane perpendicular to the force vector)		
	X	*Y*	*Z*
Loading direction (force vector)	*(BL position)*	*(AP position)*	*(vertical position)*
Vertical direction (−Z)	24.2†	16.4*	
AP direction (−Y)	24.3‡		−12.3*
BL direction (+X)		16.6‡	−12.1‡
Difference	0.1	0.2	0.2

2D-CR, 2-dimensional center of resistance; *AP*, anteroposterior; *BL*, buccolingual; *ZCR*, zone of the center of resistance.
*The AP (Y) and vertical (Z) positions of the ZCR determined in the bilateral symmetric model; †The BL position (x) of the ZCR determined in the unilateral model; ‡The additional experiments were performed in the other loading directions to quantify the discrepancies among the 2D-CRs depending on the loading directions.

method for relatively accurate localization of the ZCR. This is a useful method for visualizing model deformation and deriving quantitative results under various conditions.[27]

Recently, Viecilli et al[13] reported that geometric asymmetry of the tooth and PDL implies the existence of axes of resistance in 3 directions (AP, vertical, and BL), which do not intersect at a single point; thus, the axes do not define 3D-CR as a point, but rather as a volume, which we have called the ZCR, and the following efficient method was proposed to localize the ZCR. Because the AP and vertical positions of the ZCR in the bilateral symmetric model and the unilateral model are the same, first, the bilateral symmetric model was used to determine the AP and vertical positions of the ZCR for convenience of force application (Fig 3, *A*). Then, with reference to these positions, the most reliable corresponding BL position was determined in the unilateral model (Fig 3, *B*).

Several studies[11-13] have reported that the CR location differs with the loading direction. In the additional experiments performed in this study, the 2D-CR location in the BL loading direction was slightly more mesial and occlusal than its vertical and AP counterparts, respectively. However, the discrepancies among the 2D-CRs depending on the loading directions were too small to have a clinical impact on selecting the position of force application (Table II). Clinically, the ZCR may be simplified to a single point because the 3D-CR volume is very small. Moreover, because the force applied to a tooth constitutes a complex 3D force system, a separate 2D-CR is clinically less effective. Therefore, despite the discrepancies among the 2D-CRs depending on the loading directions, the ZCR in this study seems to be of sufficient clinical significance.

According to previous studies, the CR of a multirooted tooth is predicted to be located 1-2 mm below the furcation and between the roots in a sagittal view.[9] Similarly, in the present study, the ZCR of the mandibular first molar was located 2.3 mm below the furcation between the roots in the study model (Figs 5 and 6). Depending on the tooth size of the study model, there may be slight differences. However, in an occlusal view, the ZCR location of the mandibular molar was distobuccal with reference to the midpoint, unlike in previous studies, in which it was estimated to be at the midpoint (Figs 5 and 6).[3] In addition, the ZCR location of a mandibular molar appeared to be more apical and distobuccal than that of a maxillary molar obtained in the study by Jeong.[18] This difference may be due to morphologic differences. Choy et al[28] showed that the most occlusal and apical CR locations correspond to triangular and rectangular root shapes, respectively. A maxillary molar has a more conical root shape, an additional root on the palatal side, and the occlusal shape of a parallelogram. On the other hand, a mandibular molar has a buccolingually wide and cylindrical root shape, an additional cusp on the distal side, and the occlusal shape of a scalene quadrangle (MD width > BL width).

The results of the present study suggest that there is a tendency for the ZCR of each teeth segment to depend on the arranged position and morphology of the belonging teeth. When a premolar was added to group 2 in this study, the ZCR of the teeth segment (group 3) shifted apically, lingually, and anteriorly. This seems to be because the premolar is located more anteriorly and lingually along the arch form and is longer than the molar in the study model. This finding can be applied to predict the CR of various teeth segments with reference to the results of this study.

The 3D-FEA used in this study for evaluation of the ZCR location has many advantages, but it also has some limitations. First, FEA is a method of observing the initial tooth displacement that occurs when a force

is applied, and thus it cannot show a series of tooth movement processes with biologic responses of the periodontal tissues over time. Second, although the individual tooth movement of each tooth segment was limited by a rigid splint wire in the finite-element model, initial elastic deformation of the teeth and alveolar bone could have affected the results. Finally, the modeling was based on the average size and shape of the teeth, and thus the model may be limited for localizing the accurate customized ZCR for each patient. In this study, considering that tooth size depends on the individual, the location of the ZCR was expressed as a ratio to each reference value (root length and BL width of the mandibular first molar and sectional arch length) rather than as an absolute distance (Fig 6). In addition, depending on tooth inclination and alveolar bone height, the root length embedded in the alveolar bone may change, thus affecting the ZCR position.[29] Nevertheless, the model is advantageous in that the experimental conditions can be easily modified to reach reasonable conclusions.[21] In the future, further research will be conducted to biomechanically verify various clinical cases based on the findings of this study, and it is expected that the relationships between the ZCR and various influencing factors, such as the root shape (blunt or conical),[28] tooth inclination, and alveolar bone height,[29] will be identified. Moreover, in the future, it is expected that a more accurate patient-customized ZCR will be determined with the development of 3D finite element analysis that will reflect the morphologic variation of individual teeth and the biomechanical response of the periodontal tissues during orthodontic treatment.

The present study provides insights for clinicians who are choosing the insertion position of TADs or selecting evidence-based methods for 3D-load system applications. First, when planning the protraction of a mandibular molar for edentulous space closure, it is recommended to extend a lever arm from the tube (bracket) and apply forces on both the buccal and lingual sides to prevent side-effects (mesial tipping and rotation). If the distance from the occlusal plane to the tube (bracket) is 3 mm,[30] the ideal length of the lever arm is ~9 mm (68% of tooth length minus 3 mm). Extending 9-mm lever arms apically from the both buccal and lingual sides may be the best option, but this design may have clinical complexity for the delivery of the mechanics and induce severe discomfort for the patient because of anatomic limitations (ie, the presence of the tongue, a different level of the vestibule depth, and a different anatomic morphology of the alveolar bone). Thus, case by case, it may be beneficial to modify the length of the lever arm and apply an additional moment. In addition, clinically, a lingual protraction force using lingual attachments (eg, a lingual button) is recommended. In this case, the lingual force is recommended to be one-half the magnitude of the buccal force to prevent side-effects. This is because the ratio of the distance from the ZCR to the buccal loading point (lever arm) and the lingual loading point (lingual button) is approximately 1:2. Next, when planning the pure intrusion of an overerupted mandibular molar due to loss of the antagonist tooth,[7] it is advantageous to apply miniscrews to both the buccal and lingual sides and to allow the line of intrusive action to pass through the ZCR. However, when placing the miniscrews on the lingual side, the position of the lingual nerve should be considered when using flap surgery.[6,7] If the miniscrew is inserted in only the buccal side owing to difficulty in obtaining lingual access, the crown will be tilted buccally. In addition, pure intrusion of the mandibular first and second molar segment can be induced by applying the miniscrews buccolingually between both the molars.[6] Furthermore, when planning the intrusion of the mandibular posterior teeth segment for nonsurgical correction of a severe anterior open bite,[4,8] it is effective to concentrate the force on the first molar, where the ZCR is located. The closer the line of force is to the ZCR of the tooth, the closer it is to parallel tooth movement.

CONCLUSIONS

In this study, the ZCR location of the mandibular first molar was 0.48 of the root length from the alveolar crest level in a sagittal view and distobuccal at the AP ratio of 2:3.0 and the BL ratio of 2:2.7 in an occlusal view. The ZCRs of groups 2-4 were, respectively, 0.46, 0.50, and 0.53 of the root length of the mandibular first molar from the alveolar crest level and located slightly distobuccal at AP ratios of 2:2.3, 2:2.4, and 2:2.5 to each sectional arch length and at BL ratios of 2:1.1, 2:1.6, and 2:2.4 to the first molar's BL width. Clinically, the ZCR can be a useful reference for planning 3D movement of the mandibular posterior teeth or segments.

REFERENCES

1. Kim SJ, Sung EH, Kim JW, Baik HS, Lee KJ. Mandibular molar protraction as an alternative treatment for edentulous spaces: focus on changes in root length and alveolar bone height. J Am Dent Assoc 2015;146:820-9.
2. Mimura H. Protraction of mandibular second and third molars assisted by partial corticision and miniscrew anchorage. Am J Orthod Dentofacial Orthop 2013;144:278-89.
3. Nihara J, Gielo-Perczak K, Cardinal L, Saito I, Nanda R, Uribe F. Finite element analysis of mandibular molar protraction mechanics using miniscrews. Eur J Orthod 2015;37:95-100.
4. Sugawara J, Baik WB, Umemori M, Takahashi I, Nakasaka H, Kawamura H, et al. Treatment and posttreatment changes

following intrusion of mandibular molars with application of a skeletal anchorage system (SAS) for open bite correction. Int J Adult Orthodon Orthognath Surg 2002;17:243-53.
5. Jung MH. Treatment of severe scissor bite in a middle-aged adult patient with orthodontic mini-implants. Am J Orthod Dentofacial Orthop 2011;139:S154-65.
6. Bae SM, Kyung HM. Mandibular molar intrusion with miniscrew anchorage. J Clin Orthod 2006;40:107-8.
7. Arslan A, Ozdemir DN, Gursoy-Mert H, Malkondu O, Sencift K. Intrusion of an overerupted mandibular molar using mini-screws and mini-implants: a case report. Aust Dent J 2010;55: 457-61.
8. Freitas BV, Abas Frazão MC, Dias L, Fernandes Dos Santos PC, Freitas HV, Bosio JA. Nonsurgical correction of a severe anterior open bite with mandibular molar intrusion using mini-implants and the multiloop edgewise archwire technique. Am J Orthod Dentofacial Orthop 2018;153:577-87.
9. Smith RJ, Burstone CJ. Mechanics of tooth movement. Am J Orthod Dentofacial Orthop 1984;85:294-307.
10. Geiger ME, Lapatki BG. Locating the center of resistance in individual teeth via two- and three-dimensional radiographic data. J Orofac Orthop 2014;75:96-106.
11. Nagerl H, Burstone CJ, Becker B, Kubein-Messenburg D. Centers of rotation with transverse forces: an experimental study. Am J Orthod Dentofacial Orthop 1991;99:337-45.
12. Meyer BN, Chen J, Katona TR. Does the center of resistance depend on the direction of tooth movement? Am J Orthod Dentofacial Orthop 2010;137:354-61.
13. Viecilli RF, Budiman A, Burstone CJ. Axes of resistance for tooth movement: does the center of resistance exist in 3-dimensional space? Am J Orthod Dentofacial Orthop 2013; 143:163-72.
14. Vanden Bulcke MM, Burstone CJ, Sachdeva RCL, Dermaut LR. Location of the centers of resistance for anterior teeth during retraction using the laser reflection technique. Am J Orthod Dentofacial Orthop 1987;91:375-84.
15. Park GH, Sohn BW. The center of resistance of the maxillary anterior segment in the horizontal plane during intrusion by using laser reflection technique. Korean J Orthod 1993;23: 619-31.
16. Matsui S, Caputo AA, Chaconas SJ, Kiyomura H. Center of resistance of anterior arch segment. Am J Orthod Dentofacial Orthop 2000;118:171-8.
17. Choy K, Kim KH, Burstone CJ. Initial changes of centres of rotation of the anterior segment in response to horizontal forces. Eur J Orthod 2006;28:471-4.
18. Jeong BW. Finite element analysis on the center of resistance of the maxillary posterior teeth segment [dissertation]. Seoul: Yonsei University Graduate School; 2013.
19. Jeong GM, Sung SJ, Lee KJ, Chun YS, Mo SS. Finite-element investigation of the center of resistance of the maxillary dentition. Korean J Orthod 2009;39.
20. Sung EH, Kim SJ, Chun YS, Park YC, Yu HS, Lee KJ. Distalization pattern of whole maxillary dentition according to force application points. Korean J Orthod 2015;45:20-8.
21. Jo AR, Mo SS, Lee KJ, Sung SJ, Chun YS. Finite-element analysis of the center of resistance of the mandibular dentition. Korean J Orthod 2017;47:21-30.
22. Coolidge ED. The thickness of the human periodontal membrane. J Am Dent Assoc 1937;24:1260-70.
23. Kronfeld R. Histologic study of the influence of function on the human periodontal membrane. J Am Dent Assoc 1931;18: 1242-74.
24. Block PL. Restorative margins and periodontal health: a new look at an old perspective. J Prosthet Dent 1987;57:683-9.
25. Ziegler A, Keilig L, Kawarizadeh A, Jäger A, Bourauel C. Numerical simulation of the biomechanical behaviour of multi-rooted teeth. Eur J Orthod 2005;27:333-9.
26. Poppe M, Bourauel C, Jager A. Determination of the elasticity parameters of the human periodontal ligament and the location of the center of resistance of single-rooted teeth a study of autopsy specimens and their conversion into finite element models. J Orofac Orthop 2002;63:358-70.
27. Bourauel C, Keilig L, Rahimi A, Reimann S, Ziegler A, Jager A. Computer-aided analysis of the biomechanics of tooth movements. Int J Comput Dent 2007;10:25-40.
28. Choy K, Pae EK, Park YC, Kim KH, Burstone CJ. Effect of root and bone morphology on the stress distribution in the periodontal ligament. Am J Orthod Dentofacial Orthop 2000;117: 98-105.
29. Tanne K, Nagataki T, Inoue Y, Sakuda M, Burstone CJ. Patterns of initial tooth displacements associated with various root lengths and alveolar bone heights. Am J Orthod Dentofacial Orthop 1991;100:66-71.
30. McLaughlin RP, Bennett JC. Bracket placement with the preadjusted appliance. J Clin Orthod 1995;29:302-11.